HETEROCYCLES, Vol. 104, No. 6, 2022, pp. 1043 - 1058. © 2022 The Japan Institute of Heterocyclic Chemistry
Received, 15th February, 2022, Accepted, 9th March, 2022, Published online, 10th March, 2022
DOI: 10.3987/COM-22-14640

SUPRAMOLECULAR CHIROGENESIS IN AMIDE-LINKED BIS(ZINC PORPHYRIN): APPLICATION FOR ABSOLUTE CONFIGURATIONAL ASSIGNMENT OF CHIRAL CALBOXYLIC ACIDS AND CHIRAL AMINO ACIDS

Satoshi Hayashi,* Shiori Takeda, Takahiro Namba, Masahiro Noji, and Toshikatsu Takanami*

Meiji Pharmaceutical University, 2-522-1 Noshio, Kiyose, Tokyo 204-8588, Japan; E-mail: shayashi@my-pharm.ac.jp; and takanami@my-pharm.ac.jp

Abstract – A facile and derivatization-free method for determining the absolute configurations of a chiral carboxylic acid was developed by a supramolecular exciton-coupled circular dichroism (ECCD) protocol using the amide-linked bis(zinc porphyrin) **BP2** as a hydrogen-bonding host molecule. Using a proposed working model, the stereochemistry of various carboxylic acids and *N*-protected amino acids can be determined nonempirically.

INTRODUCTION

Optically active carboxylic acids are used a lot in medicinal chemistry, agricultural chemistry, and natural product syntheses to make useful chiral synthons.[1] Continuous effort has been made to develop an asymmetric synthesis of carboxylic acids. Therefore, determining the absolute configuration of carboxylic acids is critical.[2] Although there are several methods for determining the absolute configuration of chiral carboxylic acids, the majority of these methods require time-consuming carboxylic acid derivatization steps before analysis.[3-5] Thus, the search for a rapid and derivatization-free method has attracted the attention of a large number of researchers.

Supramolecular chirogenesis using a stereodynamic circular dichroic (CD)-sensitive host molecule has gained significant attention as a derivatization-free method for the stereochemical assignment of the chiral guest molecule. Several elaborated host molecules, developed by Setsune,[6a] Kleij,[6b] and Kondo,[6c] can be used to determine the absolute configuration of chiral carboxylic acids. By these methods, in situ-formed chiral supramolecular complexes afford characteristic induced CD spectra; thus, the stereochemistry of the chiral carboxylic acids can be empirically deduced. Although the induced CD spectra are sensitive to the chirality of the supramolecular complexes, directly correlating with the absolute stereochemistry of

the carboxylic acids is difficult. The exciton-coupled CD (ECCD) method, which uses the sign of bisignate CD spectra to directly reflect the spatial arrangement of an analyte's the chromophores, can be used to determine the absolute configuration of a chiral molecule.[7] Combining the host–guest complexation strategy with the ECCD method allows for the stereochemical assignment of chiral guest molecules without derivatization. To our knowledge, only nonempirical and derivatization-free methods for determining the absolute configuration of carboxylic acids are known: Anslyn's[8] CD-active copper complex system and Jang's[9] porphyrin-based molecular tweezer system. Therefore, the development of a rapid, nonempirical, and derivatization-free supramolecular ECCD method for chiral carboxylic acids is important.

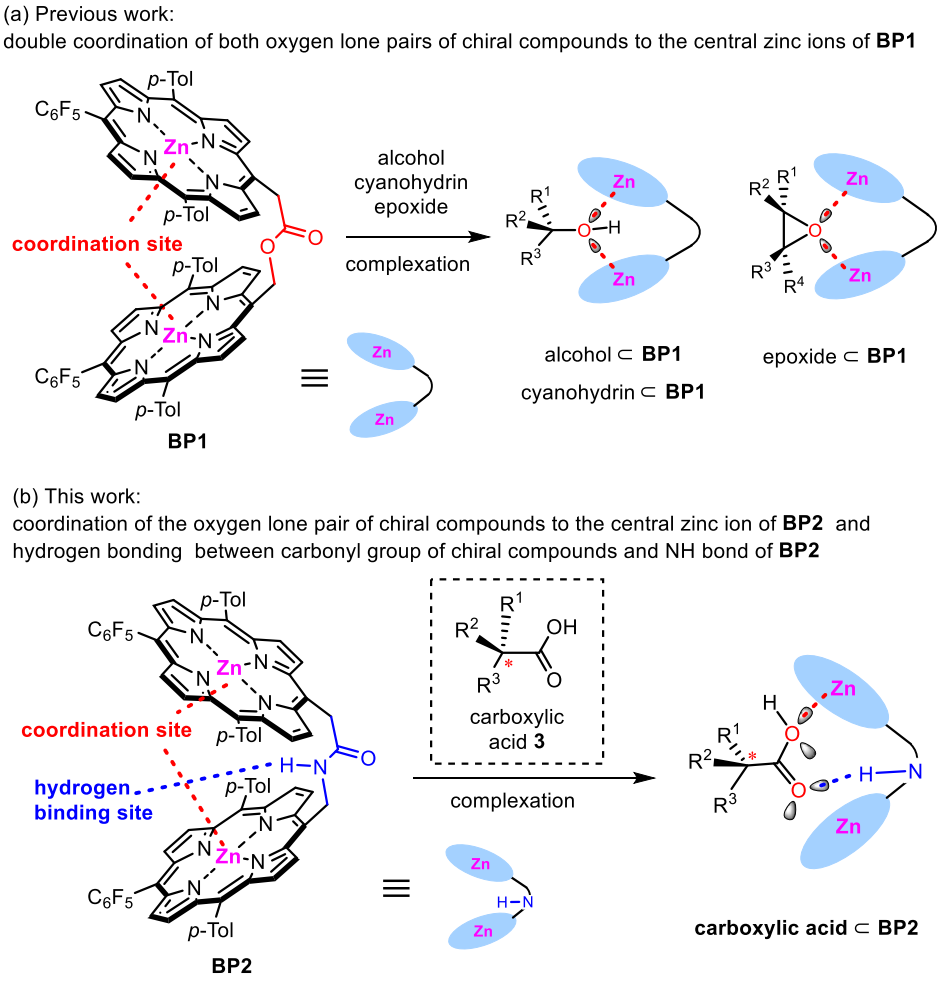

Figure 1. The host molecule's structure and a conceptual diagram of the complexation of (a) ester-linked bis(zinc porphyrin) **BP1** with monoalcohols or epoxides, and (b) amide-linked bis(zinc porphyrin) **BP2** with carboxylic acids

Recently, we described ester-linked bis(zinc porphyrin) **BP1** as a useful host molecule for the absolute configurational assignment of chiral compounds, such as alcohols,[10a] epoxides,[10b] and cyanohydrins,[10c] using the supramolecular ECCD method. The ECCD method employs the bidentate host system **BP1** as a CD-sensitive chirality probe due to its V-shaped structural motif. The double coordination of both oxygen lone pairs of the guest molecular to the two central zinc ions effectively increases the binding affinity of splayed cofacial **BP1** for monoalcohols and epoxides (Figure 1a). By employing this splayed cofacial host system strategy, we synthesized the novel amide-linked bis(zinc porphyrin) **BP2** as a hydrogen-bonding and coordination host molecule for carboxylic acids (Figure 1b). On the basis of a supramolecular ECCD protocol, we report a rapid, microscale, and nonempirical assignment for the absolute configuration of optically active carboxylic acids without chemical derivatization or additives. Additionally, a simple working model is proposed, that enables the nonempirical prediction of carboxylic acids and *N*-protected amino acids' chirality.

RESULTS AND DISCUSSION

To begin, we used ester-linked bis(zinc porphyrin) **BP1** to determine the absolute stereochemistry of a chiral carboxylic acid. Unfortunately, we observed only a trace of the ECCD spectra, and thus were unable to determine the carboxylic acid's absolute stereochemistry (Figure 2a). The low sensitivity of **BP1** is most likely due to its weak binding to carboxylic acid groups. To optimize binding, we focused on host–guest interactions via hydrogen bonding. As a result, we designed an amide-linked zinc porphyrin dimer **BP2** as a novel host molecule with hydrogen-bonding and coordination sites (Figure 1b).

As illustrated in Scheme 1, the amide-linked bis(zinc porphyrin) **BP2** is synthesized. Both the carboxylic acid and the amine parts of **Zn-6** and **Zn-8** were synthesized from **2H-4**.[10a] The carboxylic acid **Zn-6** was synthesized by the Negishi coupling of **2H-4** and the ester hydrolysis of **Zn-5**. The Pd-catalyzed cyanation[11] of **2H-4** and the subsequent reduction of **Zn-7** with DIBAL resulted in the formation of (aminomethyl)porphyrin **Zn-8**. An amide coupling of each component, **Zn-6** and **Zn-8**, with 1-ethyl-3-(3-dimethylaminopropyl)carbodiimide hydrochloride (EDC) afforded **BP2** with a 35% overall isolated yield based on starting bromoporphyrin **2H-4**.

^{1}H-NMR and UV-Vis spectroscopy were used to determine the porphyrin rings' cofacial arrangement in **BP2**. The proton signals of the β-pyrrolic positions of the porphyrin units exhibited significant upfield shifts in the NMR spectrum of **BP2**, when compared to their monomeric counterparts, **Zn-5** and **Zn-8** derivative (Figure S1, SI). The UV-Vis analysis (Figure S2, SI), the absorption spectrum of **BP2** in hexane at 25 °C showed that the Soret band was broadened with a shoulder at a wavelength (422 nm) longer than the absorption maximum (411 nm). They are quite similar to the way **BP1** behaves in the spectrum. This supports the cofacial disposition of rings in **BP2**.[10a,12]

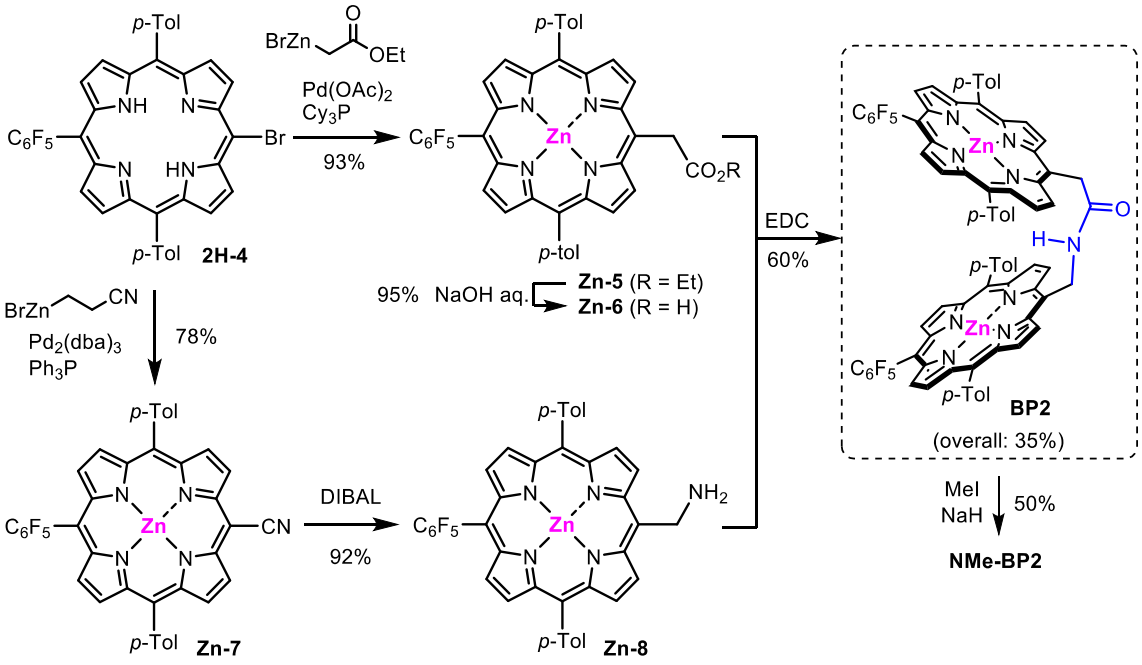

Scheme 1. Synthesis of the amide-linked host molecule **BP2** and its derivative **NMe-BP2**

The splayed cofacial **BP2** led us to suspect that **BP2** would be used as a CD-sensitive host molecule for chiral carboxylic acids. With the amide-linked **BP2** as a CD-sensitive chirality probe, the ECCD spectrum of the host molecule (2.0×10^{-6} M) was measured in the presence of 100 equiv of (*S*)-2-phenylpropionic acid (*S*)-**3a** in 5% CH_2Cl_2/*n*-hexane at 25 °C. As expected, amide-linked **BP2** provided a clear and intense bisignate CD spectrum (Figure 2b).

Then, we focused on the binding between carboxylic acids and **BP2**. The Job's continuous variation method[13] was used to determine the supramolecular complex's host–guest stoichiometry. The plot of UV-Vis spectral changes at 411 nm of these samples versus the mole fraction of **BP2** showed a peak at 0.5 (Figure S3, SI). These results indicated that **BP2** and carboxylic acid **3a** formed a 1:1 host–guest complex. Through a nonlinear least-square analysis[14] of the absorbance of the Soret bond based on a 1:1 stoichiometry, the association constant (K_{assoc}) for the supramolecular complex of amide-linked **BP2** with carboxylic acid **3a** was determined to be 1.12×10^4 M^{-1}, (Figure S4 and Figure S5, SI). The value of K_{assoc} was more than seven times greater than that of K_{assoc} for the complex of **BP1** with **3a** (1.44×10^3 M^{-1}), which indicated that amide-linked **BP2** binds with carboxylic acids more strongly than ester-linked **BP1**.

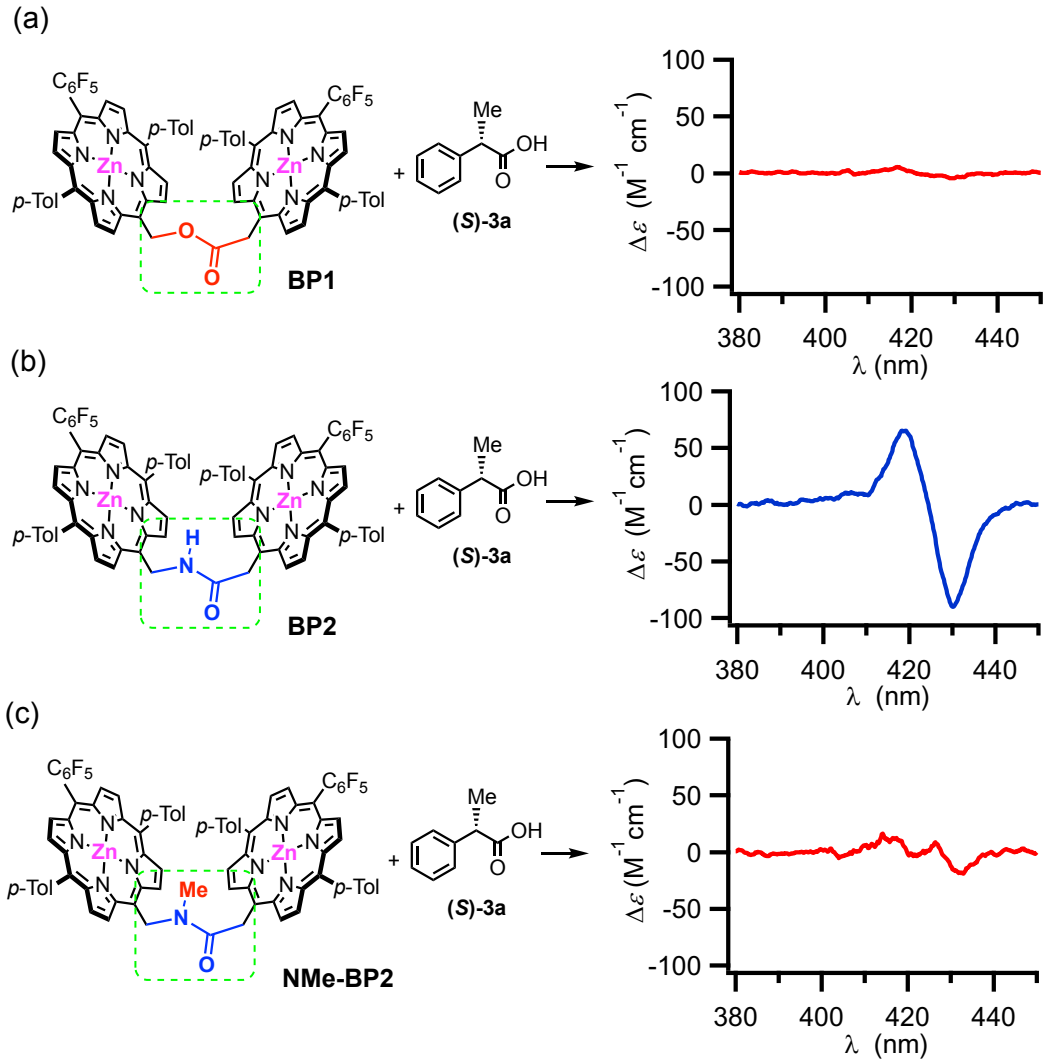

Figure 2. ECCD spectra of (a) ester-linked **BP1** and (b) amide-linked **BP2** (c) *N*-Me amide-linked **NMe-BP2** (2.0×10^{-6} M) in 5% CH_2Cl_2/*n*-hexane at 25 °C in the presence of chiral carboxylic acid **3a** (100 equiv)

The binding structure of a supramolecular complex of **BP2** and carboxylic acid was then revealed using NMR. In the absence of the host molecule, the NMR signals of methine (H^a) and methyl protons (H^b) in **3a** were observed at 3.76 and 1.50 ppm, respectively (Figure 3a). These signals shifted upfield when the zincated porphyrin **Zn-9**, a monomeric counterpart of **BP2**, was added (Figure 3b). When **BP2** was added, the signals of **3a**, H^a, and H^b, were shifted upfield more than when **Zn-9** was added (Figure 3c). Because of the strong ring current from the two porphyrin rings, carboxylic acids would be captured in the cleft between the two porphyrin rings of **BP2**, which would be in a more shielded area than in those of **Zn-9**. Additionally, to establish the hydrogen bonding between **BP2** and carboxylic acids, the **BP2** analog **NMe-BP2** lacking an NH group as a hydrogen-bonding donor was prepared via the alkylation of the NH group of **BP2** using MeI and NaH. The ECCD spectrum of **Me-BP2** was measured in the presence of 100

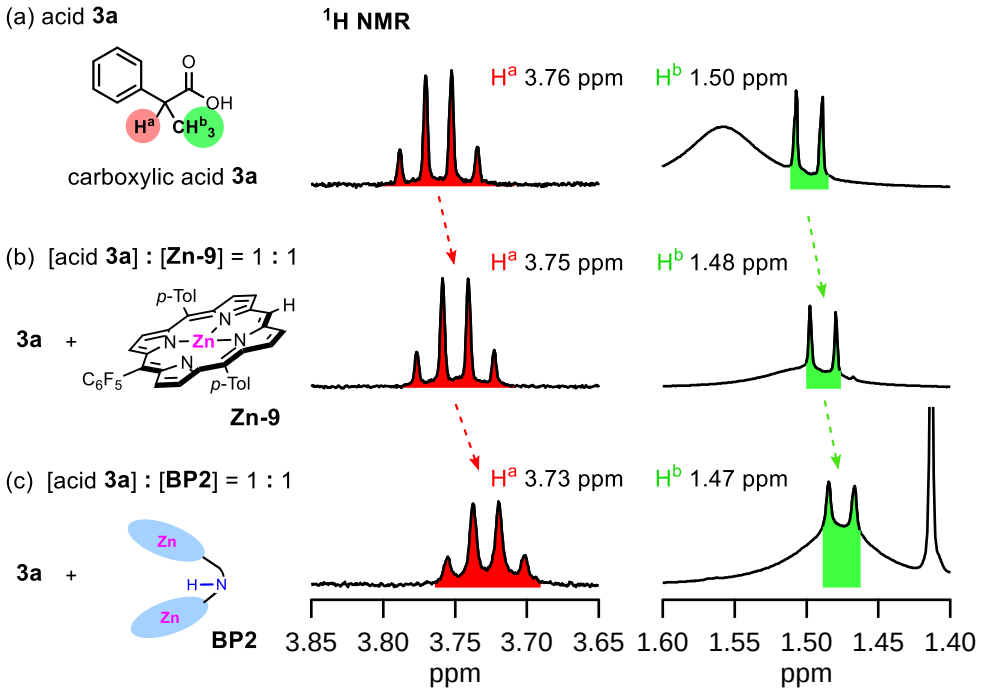

Figure 3. ^{1}H NMR spectra of (a) carboxylic acid **3a** in the presence of (b) monomeric zincated porphyirn **Zn-9** and (c) **BP2** (CD_2Cl_2, 25 °C)

equiv of (*S*)-**3a**. **NMe-BP2** yielded a multisignate CD spectrum (Figure 2c). The K_{assoc} for the supramolecular complex of **NMe-BP2** with carboxylic acid **3a** (1.87×10^3 M^{-1}) was smaller than the K_{assoc} for the complex of **BP2** with **3a** (Figure S6, SI). As a result, the hydrogen bond would be involved in the supramolecular complexation of **BP2** and carboxylic acids. Thus, **BP2** would most likely bind to carboxylic acids in a bidentate-binding mode comprised of the hydrogen bond and the coordination bond. This complex of **BP2** and carboxylic acids provided us with insights into assigning the stereochemistry of carboxylic acids. Figure 4 shows a working model for determining the absolute configuration of a chiral monocarboxylic acid to the observed ECCD spectra complexed with **BP2** in a bidentate-binding mode. A Newman-like projection of (*R*)-carboxylic acid bearing large (L), medium (M), and small (S) groups at the chiral carbon is represented in Figure 4a with the oxygen atom of the OH group in front and the chiral carbon in the back. In this working model, the lone pairs of the OH group are oriented gauche to the carbonyl C=O bond for the binding with **BP2**. With this orientation of the carboxyl group, three conformers, (*R*)-acid-i, (*R*)-acid-ii, and (*R*)-acid-iii, can be drawn (Figure 4b). When **BP2** approaches the carbonyl group of (*R*)-acid from the lowest side of steric repulsion between **BP2** and acid, (*R*)-acid-i and (*R*)-acid-ii have significant steric repulsion between the L group and the porphyrin ring of **BP2**. Therefore, the most favorable conformer for binding is (*R*)-acid-iii, whose L group is positioned in the least crowded area, opposite to the location of the binding site, and whose M group interacts with the porphyrin **P1** ring,

elevating the porphyrin ring **P1** above the **P2**. As a result, **P1** has a clockwise helicity relative to **P2**, resulting in a positive ECCD spectrum.[15]

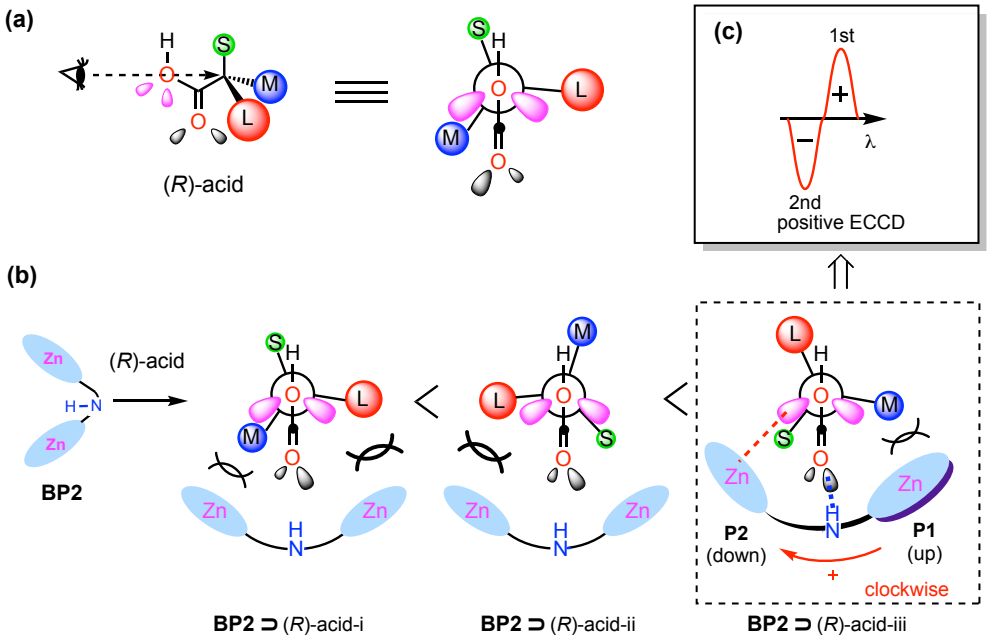

Figure 4. (a) Newman-like projection of (*R*)-acid. (b) Complexation of **BP2** with chiral carboxylic acids, as well as a proposed working model for assigning the absolute configuration of the chiral guest molecules. (c) ECCD spectrum predicted using the proposed working model.

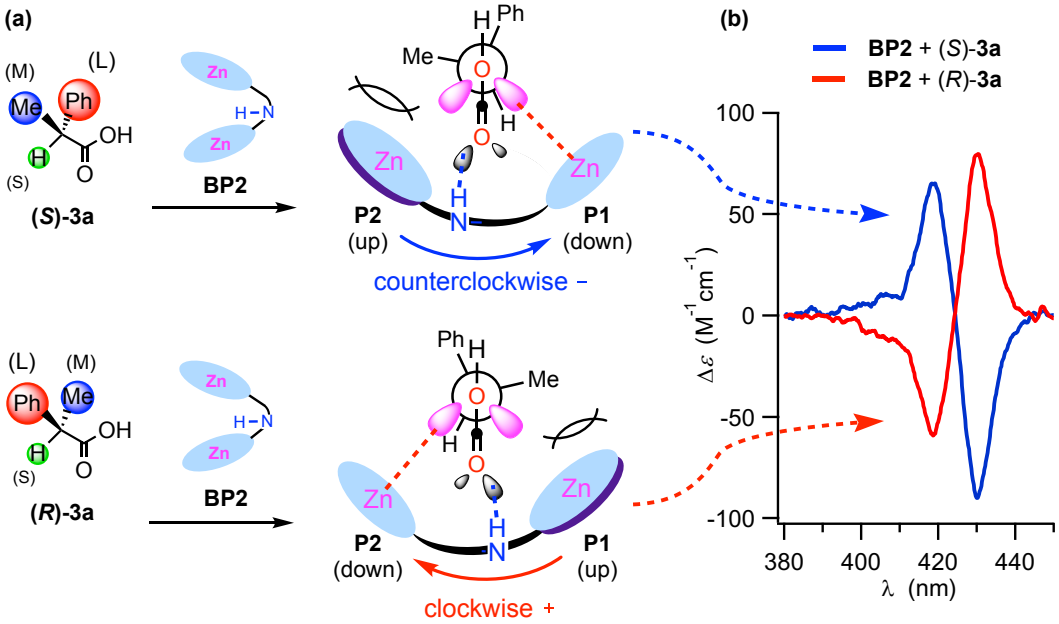

Figure 5. (a) Proposed working models for (*R*)- and (*S*)-**3a** with **BP2**. (b) Observed CD spectra of **BP2** (2.0×10^{-6} M) in the presence of **3a** (100 equiv.) in 5% CH_2Cl_2/*n*-hexane at 25 °C.

The predicted ECCD spectra of **BP2** complexed with carboxylic acid **3a**, whose substituents of Ph, Me, and H groups on the chiral carbon adopt the L, M, and S groups, respectively, were successfully applied using this working model (Figuer 5). The complexation of **BP2** with (*R*)-**3a** in 5% CH_2Cl_2/*n*-hexane at 25 °C yielded a clear bisignate positive ECCD spectrum in the Soret band, which was consistent with the working model of a steric repulsion between the Me group and the porphyrin **P1** ring, which induced the clockwise helicity of **P1** relative to **P2**. The complexation with the carboxylic acid's antipode, (*S*)-**3a**, resulted in a negative ECCD spectrum based on the counterclockwise helicity of the **P2** to **P1** rings.

Table 1. ECCD data for chiral carboxylic acids **3** with **BP2**[a]

Entry	Carboxylic acids[b,c] **3**		Predicted sign	1st λ [nm] (Δε) 2nd λ [nm] (Δε)	*A*[d]
1	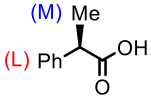	(*R*)-**3a**	pos	430 (+80) 419 (−59)	+139
2	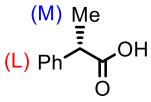	(*S*)-**3a**	neg	430 (−90) 418 (+65)	−155
3	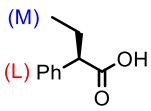	(*R*)-**3b**	pos	431 (+68) 419 (−53)	+121
4	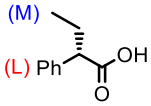	(*S*)-**3b**	neg	430 (−67) 420 (+54)	−121
5	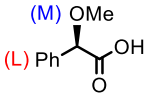	(*R*)-**3c**	pos	428 (+91) 413 (−66)	+157
6	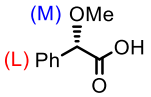	(*S*)-**3c**	neg	428 (−90) 413 (+76)	−166
7	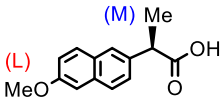	(*R*)-**3d**	pos	435 (+14) 426 (−20)	+34
8	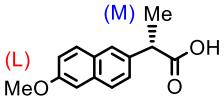	(*S*)-**3d**	neg	435 (−12) 426 (+28)	−40

[a] All CD measurements were performed with 2.0 μM of **BP2** in 5% CH_2Cl_2/*n*-hexane at 25 °C; 100 equiv of carboxylic acid **3** was used. [b] All substrates were >99% ee. [c] The letters (L) and (M) denote sterically larger and medium groups, respectively; the M and L groups are assigned based on their conformational energies, or *A* value (Figures S7–10, SI). [d] $A = \Delta\varepsilon_{1st} - \Delta\varepsilon_{2nd}$.

The scope of surpramolecular chirogenesis was investigated using **BP2** and a variety of chiral carboxylic acids as CD-sensitive host molecules. As shown in Table 1, all the carboxylic acids examined upon complexation with **BP2** exhibited the corresponding ECCD signals with acceptable amplitudes in 5% CH_2Cl_2/*n*-hexane at 25 °C. In all cases, the observed ECCD couplet of the complexes of **BP2** and carboxylic acids agreed with the predicted ECCD sign based on the bidentate-binding mode in Figure 4 and Figure 5. In this system, the difference in steric bulk of the Ph and alkyl groups in **3a** and **3b** could be clearly distinguished (Table 1, entries 1–4, and Figures S7–S8, SI). The presence of an ether functional group such as the MeO group in **3c**, which could coordinate with zinc porphyrin, did not disturb the analysis (Table 1, entries 5 and 6, and Figure S9, SI). Also, a large 6-methoxy-2-naphthyl group in **3d** was used for chiral sensing (Table 1, entries 7 and 8, and Figure S10, SI).

To further demonstrate the utility of this chiroptical protocol, the correlation between the amplitude of the ECCD signal ($A = \Delta\varepsilon_{(1st)} - \Delta\varepsilon_{(2nd)}$) and the ee of carboxylic acid **3a** was examined. The measurements were performed using 100 equiv of (*R*)-**3a** (99% ee) ~ (*S*)-**3a** (99% ee) in 5% CH_2Cl_2/*n*-hexane at 25 °C (Figure 6a). As expected, an excellent linear relationship was obtained between the ECCD amplitude and the % ee of carboxylic acid **3a**, with linear regression yielding a correlation coefficient of 0.998 (Figure 6b).

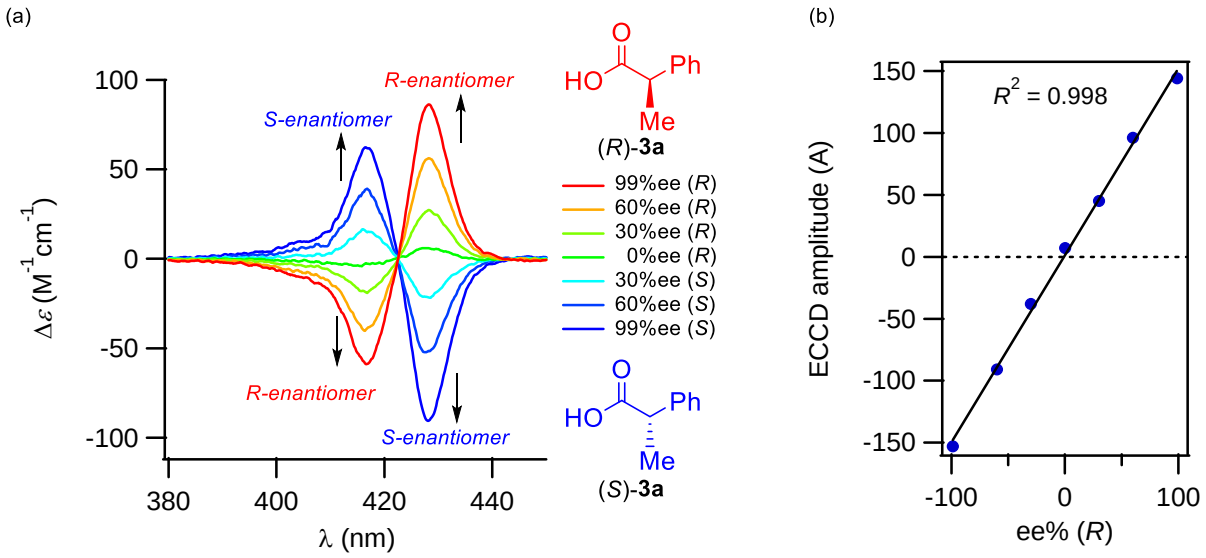

Figure 6. (a) ECCD spectra of **BP2** (2.0×10^{-6} M) complexed with **3a** (100 equiv) at different enantiomeric excesses (ECCD spectra were recorded in 5% CH_2Cl_2/*n*-hexane at 25 °C). (b) Plot of ECCD amplitude ($A = \Delta\varepsilon_{(430\ nm)} - \Delta\varepsilon_{(419\ nm)}$) versus % ee of (*R*)-**3a** in complex with **BP2**.

We then focused on *N*-protected amino acid derivatives. **BP2** was capable of binding *N*-Boc-protected amino acid (*R*)-**10a** under the same conditions, yielding the expected negative ECCD spectrum based on the binding mode explained (Table 2, entry 1, and Figure S11, SI). Whereas the positive signal can be

observed for enantiomer (*S*)-**10a** (Table 2, entry 2, and Figure S11, SI). Thus, the **BP2** host system also works well for *N*-protected amino acid derivatives. Upon complexation with **BP2**, *N*-Boc-protected amino acids **10b** and **10c** resulted in the corresponding bisignate ECCD spectra, which could also be rationalized in terms of the binding model proposed (Table 2, entries 3–6, and Figures S12–S13, SI). Not only are *N*-Boc-protected amino acids compatible with the **BP2** host system, but also with *N*-Cbz-protected amino acids, such as *N*-Cbz-phenylalanine **10d** (Table 2, entries 7 and 8, and Figure S14, SI).

Table 2. ECCD data for chiral *N*-protected amino acids **10** with **BP2**[a]

Entry	*N*-Protected amino acids[b,c] **10**		Predicted sign	1st λ [nm] (Δε) 2nd λ [nm] (Δε)	*A*[d]
1	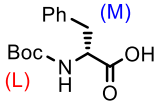	(*R*)-**10a**	neg	426 (−165) 415 (+104)	−269
2	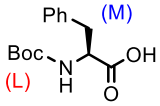	(*S*)-**10a**	pos	426 (+155) 415 (−85)	+240
3	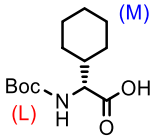	(*R*)-**10b**	neg	428 (−583) 417 (+412)	−995
4	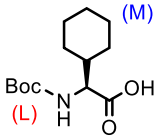	(*S*)-**10b**	pos	428 (+624) 426 (−427)	+1051
5	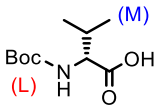	(*R*)-**10c**	neg	428 (−372) 415 (+260)	−632
6	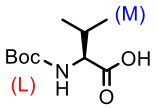	(*S*)-**10c**	pos	428 (+353) 417 (−235)	+588
7	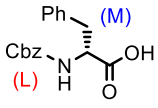	(*R*)-**10d**	neg	429 (−77) 413 (+59)	−136
8	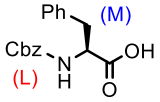	(*S*)-**10d**	pos	430 (+85) 412 (−65)	+150

[a] All CD measurements were performed with 2.0 μM of **BP2** in 5% CH_2Cl_2/*n*-hexane at 25 °C; 100 equiv of *N*-protected amino acid **10** was used. [b] All substrates were >99% ee. [c] The letters (L) and (M) denote sterically larger and medium groups, respectively; the M and L groups are assigned based on the length of the substituents (Figures S11–14, SI). [d] $A = \Delta\varepsilon_{1st} - \Delta\varepsilon_{2nd}$.

CONCLUSION

In summary, we have developed a simple and derivatization-free method for determining the absolute configurations of chiral monocarboxylic acids by the supramolecular ECCD method using the new amide-linked bis(zinc porphyrin) **BP2** as a hydrogen-bonding host molecule. **BP2** is easily synthesized through the amide coupling of acid and amine counterparts. Both of these compounds can be synthesized using readily available synthetic intermediates, such as a bromoporphyrin derivative. At the same time, UV-Vis and NMR spectroscopy revealed that the chiral carboxylic acid was incorporated between two porphyrin rings to form a 1:1 host–guest complex that reflects the carboxylic acid's stereochemistry. CD studies on the structural analog of **BP2** showed that the bisignate ECCD output required the zinc porphyrin core and the amide functionality's NH group. From observed ECCD spectra, we propose a simple working model for nonempirically predicting the stereochemistry of various monocarboxylic acids and *N*-protected amino acids. We are currently investigating the possibility of expanding the current method to include more functional groups.

EXPERIMENTAL

The ^{1}H and ^{13}C NMR spectra were recorded at RT using perdeuterated solvents as internal standards on a JEOL JNM ECZ-500, a JEOL JNM ECS-400, and a JEOL JNM AL-300 spectrometer. The chemical shifts of the ^{1}H- and ^{13}C-NMR spectra are given in ppm relative to the residual protonated solvent and solvent $CHCl_3$ (δ = 7.24) for ^{1}H-NMR and relative to the central resonance of $CDCl_3$ (δ = 77.0) for ^{13}C NMR. ^{19}F-NMR spectra were recorded at RT on a JEOL JNM ECZ-500, and a JEOL JNM ECS-400 spectrometer using benzotrifluoride as an external standard. The chemical shift values are expressed as δ values (ppm) and the couple constant values (*J*) are given in Hertz (Hz). The following abbreviations were used for signal multiplicities: s, singlet; d, doublet; t, triplet; q, quartet; m, multiplet; and br, broad. UV-visible spectra were recorded on a JASCO V-660 dual-beam grating spectrophotometer with a 1 cm cell. IR spectra were recorded on a JASCO FT/IR-4100 spectrophotometer. The JEOL JMS-700 spectrometer was used to collect the mass spectroscopic data. Optical rotations were measured on the JASCO P-1020 polarimeter. The CD spectra were recorded on a JASCO J-820 spectrophotometer with a 1 cm cell. Reactions involving moisture-sensitive reagents were carried out under an argon atmosphere using standard vacuum line techniques and glassware that was flame-dried and cooled under argon before use. Dry THF was purchased for the reactions and used without further desiccation. **2H-4**, **Zn-5**, **Zn-6**, **Zn-9**, and bis(zinc porphyrin) **BP1** were synthesized using the methods described in the literature.[10a] Other chemicals were purchased from commercial sources and used as received unless otherwise stated. Commercially available chiral carboxylic acids and amino acid derivatives were used without further purification.

[5-Cyano-15-pentafluorophenyl-10,20-di(*p*-tolyl)porphyrinato]zinc(II) (Zn-7): According to the method described in the literature.[11] An oven-dried 25 mL sealable Schlenk flask equipped with a magnetic stirring bar was charged with *meso*-bromoporphyrin **2H-4**[10a] (28.0 mg, 38.1 μmol), $Pd_2(dba)_3$ (5.20 mg, 5.68 μmol), and triphenylphosphine (2.60 mg, 9.91 μmol). The reaction vessel was evacuated and flushed with argon (three times), and then dry dioxane (10 mL) was added. At room temperature, 2-cyanoethylzinc bromide was added to the solution (0.5 M in THF, 1 mL, 0.500 mmol). The mixture was heated at 110 °C for 12 h under argon and then allowed to cool to room temperature. The reaction mixture was diluted with CH_2Cl_2 (10 mL) and washed with aqueous NH_4Cl and brine. The organic layer was dried over $MgSO_4$ and filtered. The filtrate was concentrated in vacuo. The residue was purified by column chromatography on silica gel (*n*-hexane/THF, 4:1) followed by recrystallization from CH_2Cl_2/*n*-hexane to give **Zn-7** (20.0 mg, 71%) as a purple solid: ^{1}H-NMR (THF-d_8, 400 MHz) δ: 9.62 (2H, d, J = 4.4 Hz), 9.05 (2H, d, J = 4.4 Hz), 8.95 (2H, d, J = 4.4 Hz), 8.91 (2H, d, J = 4.4 Hz), 8.08 (4H, m), 7.61 (4H, m), 2.71 (6H, s); ^{13}C-NMR (THF-d_8, 100 MHz) δ: 152.6, 152.2, 151.8, 149.7, 147.4 (2C, d, J_{CF} = 243.3 Hz), 144.2 (1C, d, J_{CF} = 269.8 Hz), 140.1, 138.4 (2C, d, J_{CF} = 254.1 Hz), 138.3, 135.2, 134.9, 133.7, 131.2, 130.5, 128.0, 124.1, 122.8, 118.1 (1C, t, J_{CF} = 21.5 Hz), 106.0, 86.8, 21.4; ^{19}F-NMR ($CDCl_3$, 376 MHz) δ: −132.0 (2F, dd, J_{FF} = 23.6, 8.6 Hz), −147.3 (1F, t, J_{FF} = 21.3 Hz), −156.9 (2F, td, J_{FF} = 21.8, 7.3 Hz); UV-Vis (CH_2Cl_2) λ_{max} (log ε) 416.0 (5.6), 548.5 (4.1), 586.5 (4.2) nm; IR (KBr) 2922, 2231, 1496, 1342, 1072, 991, 793 cm^{-1}; HRMS (FAB) [M^+] calcd for $C_{41}H_{22}F_5N_5Zn$: 743.1087, found 743.1087.

[5-(Aminomethyl)-15-pentafluorophenyl-10,20-di(*p*-tolyl)porphyrinato]zinc(II) (Zn-8): A charge of **Zn-7** (74.5 mg, 100 mol) was charged into an oven-dried 100 mL two-necked flask equipped with a magnetic stirring bar. The reaction vessel was evacuated and flushed three times with argon, and then 60 mL of dry toluene was added. The solution was diluted with diisobutylaluminum hydride (1 M in toluene, 2.00 mL, 2.00 mmol) at room temperature. At 100 °C, the mixture was stirred for 6 h. After the reaction was completed, the mixture was cooled to 0 °C and NaF (2.00 mmol, 84.0 mg) and H_2O (40 mL) were added. The mixture was vigorously stirred for 0.5 h. The reaction mixture was filtered through a filter paper, diluted with CH_2Cl_2 (20 mL), and washed with aqueous NH_4Cl and brine. Vacuolation was used to concentrate the organic layer. The resulting solid was purified by recrystallization from CH_2Cl_2/*n*-hexane to give **Zn-8** (69.0 mg, 92%) as a purple solid: IR (KBr) 3395, 1654, 1560, 1524, 1490, 1458, 1439, 1387, 1065, 1004, 846, 788 cm^{-1}; HRMS (EI) [M^+] calcd for $C_{41}H_{26}F_5N_5Zn$: 747.1400, found 747.1396; UV-Vis (CH_2Cl_2) λ max (log ε) 420.5 (5.6), 551.5 (4.5), 600.6 (4.3), 623.5 (4.3) nm. Due to the compound's low solubility, NMR data could not be obtained. Additionally, the structure of **Zn-8** was further characterized as a propionylamide derivative. At room temperature, EDC (16.0 mg, 83.5 μmol) was added to a mixture of **Zn-8** (37.2 mg, 49.7 μmol) and propionic acid (3.3 μL, 44 μmol) in THF (15

mL). After stirring for 19 h at room temperature, the solution was diluted with THF/Et_2O (2:1, 60 mL) and washed with brine. The organic layer was dried over $MgSO_4$ and filtered. The filtrate was concentrated under reduced pressure. The residue was purified by column chromatography on silica gel (*n*-hexane/THF, 4:1) followed by recrystallization from CH_2Cl_2/*n*-hexane to give a propionylamide derivative (24.1 mg, 60%) as a purple solid: ^{1}H-NMR ($C_6D_5CD_3$, 500 MHz) δ: 9.37 (2H, d, J = 4.6 Hz), 9.04 (2H, d, J = 4.6 Hz), 9.04 (2H, d, J = 4.6 Hz), 8.69 (2H, d, J = 4.6 Hz), 8.09 (4H, d, J = 7.6 Hz), 7.41 (4H, d, J = 7.6 Hz), 6.34 (2H, s), 5.66 (1H, br s), 2.52 (6H, s), 1.43 (2H, q, J = 6.7 Hz), 0.72 (3H, t, J = 6.7 Hz); ^{13}C-NMR ($CDCl_3$, 100 MHz) δ: 171.6, 150.9, 150.6, 150.1, 149.4, 146.5 (2C, d, J_{CF} = 251.1 Hz), 141.5 (1C, d, J_{CF} = 242.5 Hz), 139.3, 137.4, 137.1 (2C, d, J_{CF} = 236.7 Hz), 134.4, 133.7, 133.4, 129.7, 129.0, 127.4, 125.5, 121.8, 117.3, 114.4, 42.6, 30.3, 21.5, 9.2; ^{19}F-NMR ($CDCl_3$, 376 MHz) δ: −137.1 (2F, dd, J_{FF} = 24.1, 8.0 Hz), −153.2 (1F, t, J_{FF} = 21.3 Hz), −162.4 (2F, td, J_{FF} = 22.7, 7.7 Hz); IR (KBr) 3440, 2958, 1639, 1519, 1340, 1211, 1074, 991, 939, 796 cm^{-1}; UV-Vis (*n*-hexane in 5% CH_2Cl_2) λ_{max} (log ε) 395.0 (4.5) 414.5 (5.6), 545.0 (4.1), 579.0 (3.6) nm; HRMS (EI) [M^+] calcd for $C_{44}H_{30}F_5N_5OZn$: 803.1662, found 803.1670.

Amide-linked bis(zinc porphyrin) BP2: At room temperature, EDC (16.7 mg, 87.1 μmol) was added to a mixture of **Zn-8** (20.9 mg, 27.9 μmol) and **Zn-6**[10a] (22.8 mg, 29.3 μmol) in THF (8 mL). The solution was diluted with THF/Et_2O (2:1, 60 mL) and washed with brine after stirring for 20 h at room temperature. The organic layer was dried and filtered over $MgSO_4$. In vacuo, the filtrate was concentrated. The residue was purified by column chromatography on silica gel (*n*-hexane/THF, 4:1) followed by recrystallization from CH_2Cl_2/*n*-hexane to give **BP2** (24.0 mg, 60%) as a purple solid: ^{1}H-NMR ($C_6D_5CD_3$, 400 MHz) δ: 8.78 (2H, d, J = 4.9 Hz), 8.68 (2H, d, J = 4.9 Hz), 8.46 (2H, d, J = 4.9 Hz), 8.46 (2H, d, J = 4.9 Hz), 8.34 (2H, d, J = 4.4 Hz), 8.33 (2H, d, J = 4.4 Hz), 7.85 (2H, s, br), 7.77 (2H, s, br), 7.65 (4H, d, J = 7.8 Hz), 7.55 (4H, d, J = 7.3 Hz), 7.31 (4H, d, J = 7.3 Hz), 7.20 (4H, d, J = 7.8 Hz), 4.98 (1H, s), 4.48 (2H, s), 3.09 (2H, s), 2.60 (6H, s), 2.57 (6H, s); ^{13}C-NMR ($C_6D_5CD_3$) δ: 169.16, 150.60, 150.56, 150.53, 150.52, 149.69, 149.68, 149.38, 149.20, 146.92 (2C, d, J_{CF} = 239.2 Hz), 141.81 (1C, d, J_{CF} = 250.8 Hz), 140.26, 140.15, 137.70 (2C, d, J_{CF} = 250.8 Hz), 137.06, 134.65, 134.54, 133.36, 133.28, 132.87, 132.62, 127.48, 127.39, 121.53, 121.29, 118.30, 112.77, 110.52, 101.45, 101.27, 66.95, 30.55, 21.40, 21.37. ^{19}F-NMR ($C_6D_5CD_3$) δ: −137.63 (2F, d, J_{FF} = 23.4 Hz), −137.64 (2F, d, J_{FF} = 23.4 Hz), −153.95 (1F, t, J_{FF} = 20.7 Hz), −153.98 (1F, t, J_{FF} = 20.7 Hz), −163.21 (2F, t, J_{FF} = 20.2 Hz), −163.21 (2F, t, J_{FF} = 20.2 Hz); IR (KBr) 3397, 2923, 1633, 1521, 1492, 1340, 1209, 1076, 989, 939 cm^{-1}; UV-Vis (CH_2Cl_2) λ_{max} (log ε) 409.0 (5.8), 546.5 (4.7) nm; HRMS (ESI) [M^+] calcd for $C_{83}H_{49}F_{10}N_9OZn_2$: 1505.2483, found 1505.2483.

BP2 analog **(NMe-BP2):** Charged with **BP2** (20.0 mg, 13.3 mol) in an oven-dried 20 mL two-necked flask equipped with a magnetic stirring bar and rubber septum. The reaction vessel was evacuated and

flushed three times with argon before adding dry THF (6 mL). At 0 °C, three portions of NaH (60% dispersion in paraffin liquid, 7.00 mg, 175 μmol) were added to the solution and the mixture was stirred for 15 min. Then, CH_3I (10 μL, 161 μmol) was added dropwise to the mixture, and the reaction mixture was stirred until completion as monitored by TLC (17 h). After the reaction was completed, 30 mL of water was added to the reaction mixture, and the solution was diluted with EtOAc. The organic layer was washed with water and brine, then dried and filtered over anhydrous $MgSO_4$. The filtrate was concentrated in vacuo. The residue was purified by column chromatography on silica gel (*n*-hexane/THF, 4:1) followed by recrystallization from CH_2Cl_2/*n*-hexane to give **NMe-BP2** (8.00 mg, 40%) as a purple solid: ^{1}H-NMR ($C_6D_5CD_3$) δ: 9.79 (2H, d, J = 4.8 Hz), 9.72 (2H, d, J = 4.8 Hz), 9.03 (2H, d, J = 4.8 Hz), 8.98 (2H, d, J = 4.6 Hz), 8.94 (2H, d, J = 4.8 Hz), 8.82 (2H, d, J = 4.9 Hz), 8.69 (2H, d, J = 4.8 Hz), 8.63 (2H, d, J = 4.8 Hz), 8.03 (4H, d, J = 7.5 Hz), 7.94 (4H, d, J = 7.9 Hz), 7.39 (4H, d, J = 7.9 Hz), 7.30 (4H, d, J = 7.5 Hz), 3.26 (2H, s), 3.23 (2H, s), 2.53 (6H, s), 2.49 (6H, s), 1.35 (3H, s); ^{13}C-NMR (CD_2Cl_2, THF-d_8) δ: 171.5, 151.2, 151.1, 150.7, 150.4, 150.2, 150.0, 149.0, 148.9, 146.33 (d, J = 245.4 Hz), 146.27 (d, J = 244.4 Hz), 141.4 (d, J = 244.4 Hz), 141.2 (d, J = 249.2 Hz), 139.5, 137.3 (d, J = 247.3 Hz), 137.1 (d, J = 247.3 Hz), 137.0, 135.8, 134.2, 134.2, 132.9, 132.7, 132.3, 132.1, 131.8, 131.2, 129.1, 128.8, 127.9, 126.9, 126.8, 125.1, 125.0, 121.1, 121.0, 114.4, 114.0, 106.0, 100.5, 33.8, 29.75, 29.69, 20.94, 20.82; ^{19}F-NMR (CD_2Cl_2, THF-d_8) δ: −138.25 (2H, dd, J_{FF} = 26.8, 7.8 Hz), −138.32 (2H, dd, J_{FF} = 25.0, 7.8 Hz), −155.00 (1H, td, J_{FF} = 20.3, 9.2 Hz), −155.24 (1H, t, J_{FF} = 20.7 Hz), −163.76 (2H, td, J_{FF} = 18.1, 6.9 Hz), −163.87 (2H, td, J_{FF} = 23.3, 6.9 Hz); IR (KBr) 3122, 3019, 2921, 1654, 1519, 1492, 1074, 989, 939, 796 cm^{-1}; UV-Vis (CH_2Cl_2) λ_{max} (log ε) 413.0 (5.6), 419.0 (5.7), 546.5 (4.5) nm; HRMS (EI) [M^+] calcd for $C_{84}H_{51}F_{10}N_9OZn_2$: 1519.2640, found 1519.2632.

ACKNOWLEDGMENTS

This work was supported by JSPS KAKENHI Grant Number JP21K06463.

REFERENCES AND NOTES

1. C. Lamberth and J. Dinges, 'Bioactive Carboxylic Compound Classes Pharmaceutical and Agrochemicals,' Wiley-VCH, Weinheim, 2016.
2. Review and selected examples of asymmetric synthesis of carboxylic acid, see: (a) S.-F. Zhu and Q.-L. Zhou, *Acc. Chem. Res.*, 2017, **50**, 988; (b) C. E. Stivala and A. Zakarian, *J. Am. Chem. Soc.*, 2011, **133**, 11936; (c) K. C. Miles, M. L. Abrams, C. R. Landis, and S. S. Stahl, *Org. Lett.*, 2016, **18**, 3590; (d) K. Yu, P. Lu, J. J. Jackson, T.-A. D. Nguyen, J. Alvarado, C. E. Stivala, Y. Ma, K. A. Mack, T. W. Hayton, D. B. Collum, and A. Zakarian, *J. Am. Chem. Soc.*, 2017, **139**, 527; (e) S. E. Shockley, J. C. Hethcox, and B. M. Stoltz, *Angew. Chem. Int. Ed.*, 2017, **56**, 11545; (f) K. Yu, B.

Miao, W. Wang, and A. Zakarian, *Org. Lett.*, 2019, **21**, 1930; (g) R. Niu, Y. He, and J.-B. Lin, *Org. Biomol. Chem.*, 2022, **20**, 37.

3. Mosher's and related method, see: (a) T. Yabuuchi and T. Kusumi, *J. Org. Chem.*, 2000, **65**, 397; (b) M. J. Ferreiro, S. K. Latypov, E. Quiñoá, and R. Riguera, *J. Org. Chem.*, 2000, **65**, 2658; (c) M. Kurosu and K. Li, *Org. Lett.*, 2009, **11**, 911.
4. CD measurements after derivatization, see: (a) S. Superchi, R. Bisaccia, D. Casarini, A. Laurita, and C. Rosini, *J. Am. Chem. Soc.*, 2006, **128**, 6893; (b) J. Zhang, W. Sheng, H. Gholami, T. Nehira, and B. Borhan, *Chirality*, 2018, **30**, 141.
5. Nonempirical ECCD method with derivatization, see: (a) G. Proni, G. Pescitelli, X. Huang, N. Q. Quraishi, K. Nakanishi, and N. Berova, *Chem. Commun.*, 2002, 1590; (b) Q. Yang, C. Olmsted, and B. Borhan, *Org. Lett.*, 2002, **4**, 3423; (c) G. Proni, G. Pescitelli, X. Huang, K. Nakanishi, and N. Berova, *J. Am. Chem. Soc.*, 2003, **125**, 12914; (d) M. Tanasova, C. Vasileiou, O. O. Olumolade, and B. Borhan, *Chirality*, 2009, **21**, 374; (e) M. Tanasova and B. Borhan, *Eur. J. Org. Chem.*, 2012, 3261; (f) M. Tanasova, M. Anyika, and B. Borhan, *Angew. Chem. Int. Ed.*, 2015, **54**, 4274.
6. Empirical CD system, see: (a) J. M. Lintuluoto, K. Nakayama, and J. Setsune, *Chem. Commun.*, 2006, 3492; (b) S. J. Wezenberg, G. Salassa, E. C. Escudero-Adán, J. Benet-Buchholz, and A. W. Kleij, *Angew. Chem. Int. Ed.*, 2011, **50**, 713; (c) K. Osawa, H. Tagaya, and S. Kondo, *J. Org. Chem.*, 2019, **84**, 6623.
7. Reviews for ECCD method, see: (a) N. Berova, G, Pescitelli, A. G. Petrovic, and G. Proni, *Chem. Commun.*, 2009, 5958; (b) C. Wolf and K. W. Bentley, *Chem. Soc. Rev.*, 2013, **42**, 5408; (c) H. Gholami, D. Chakraborty, J. Zhang, and B. Borhan, *Acc. Chem. Res.*, 2021, **54**, 654.
8. Derivatization-free nonempirical ECCD method, see: L. A. Joyce, M. S. Maynor, J. M. Dragna, G. M. da Cruz, V. M. Lynch, J. W. Canary, and E. V. Anslyn, *J. Am. Chem. Soc.*, 2011, **133**, 13746.
9. Derivatization-free nonempirical ECCD method for carboxylic acids using bis-porphyrin, see: H. Yoon, C.-H. Lee, and W.-D. Jang, *Chem. Eur. J.*, 2012, **18**, 12479.
10. Derivatization-free nonempirical ECCD method for mono-functional chiral compounds using bis-porphyrin, see: (a) S. Hayashi, M. Yotsukura, M. Noji, and T. Takanami, *Chem. Commun.*, 2015, **51**, 11068; (b) S. Takeda, S. Hayashi, M. Noji, and T. Takanami, *J. Org. Chem.*, 2019, **84**, 645; (c) S. Hayashi, S. Takeda, M. Noji, and T. Takanami, *Heterocycles*, 2019, **98**, 1215.
11. Pd-Catalyzed cyanation of bromoporphyrins, see: T. Takanami, M. Hayashi, H. Chijimatsu, W. Inoue, and K. Suda, *Org. Lett.*, 2005, **7**, 3937.
12. (a) M. Kasha, H. R. Rawls, and M. A. El-Bayoumi, *Pure Appl. Chem.*, 1965, **11**, 371; (b) B. Tu, B. Ghosh, and D. A. Lightner, *J. Org. Chem.*, 2003, **68**, 8950 and references cited therein.
13. Job's plot, see: (a) E. J. Olson and P. Bühlmann, *J. Org. Chem.*, 2011, **76**, 8406; (b) F. Ulatowski, K.

Dąbrowa, T. Bałakier, and J. Jurczak, *J. Org. Chem.*, 2016, **81**, 1746.

14. A nonlinear curve-fitting method for obtaining K_{assoc}, see: Y. Shoji, K. Tashiro, and T. Aida, *J. Am. Chem. Soc.*, 2006, **128**, 10690.
15. If the orientation of the chromophore is clockwise, the CD spectra shows positive first (at longer wavelength) cotton effect and a negative second cotton effect (defined as positive), see: (a) N. Harada and K. Nakanishi, 'Circular Dichroic Spectroscopy: Exciton Coupling in Organic Stereochemistry,' University Science Books, Mill Valley, 1984; (b) N. Berova, K. Nakanishi, and R. W. Woody, 'Circular Dichroism, Principles and Applications 2nd Edn.,' Wiley, New York, 2000; (c) N. Kobayashi, A. Muranaka, and J. Mack, 'Circular Dichroism and Magnetic Circular Dichroism Spectroscopy for Organic Chemists,' RSC, Cambridge, 2012.